γγ COLLISIONS: EXPERIMENTAL ASPECTS

J.H. Field
DESY, Hamburg

1. Introduction and Summary

This review is divided into 4 sections. In section 1 the problem of separating 1γ and 2γ processes is rediscussed in the light of new theoretical expectations of high p_t hadron production from jets in 2γ processes[1-4]. Here there is some overlap with P. Landshoff's review, but as a rather complete monte carlo study of single particle inclusive production in both 1γ and 2γ processes has now been done[5] some quite firm conclusions can be reached. In spite of the 20 times larger ratio of 2γ/1γ cross-sections at LEP, as compared to PEP or PETRA, no problem is expected in separating processes with hadronic final states. Heavy lepton production is also considered in section 1 and here the conclusions are not so optimistic, particularly if several heavy leptons exist within the energy range of the machine. More work is needed here. Section 2 considers 3 potentially interesting fields of 2γ physics: (i) jet production, (ii) deep inelastic γγ scattering, (iii) production of C = +1 resonances. Experimental signatures are discussed and rates are given. In section 3 tagging is discussed. The main points here are: a) Tagging efficiency, in particular the effect of vector meson propagators[6], which may suppress the tagging efficiency for some 2γ processes by an order of magnitude or more as compared with previous assumptions. b) Backgrounds. These include the "intrinsic" background resulting from π/e misidentification, as well as various external backgrounds resulting in production of electrons at small angles. By far the most serious of the latter is beam-gas bremsstrahlung, which imposes quite severe constraints on the vacuum in the LEP straight sections, if tagging is to be a viable proposition. Finally, in section 4, single particle inclusive production of hadrons in various 1γ and 2γ processes are shown for different angular acceptance regions of a practical detector, and some features of a possible 2γ detector for LEP are summarized. More detailed discussions of the problems of 2γ detector design are presented elsewhere[7,8].

2. Separation of 1γ and 2γ Processes

2.1 Hadronic Final States

A number of different possible processes resulting in jets in the final state are shown in Fig. 1a)-g). Of these, the dominant contribution at high p_t is expected to come from the QED graph, Fig. 1a). The cross-section for this graph, when the quarks have large p_t, is expected [1,3] to be related to 2γ production of μ pairs:

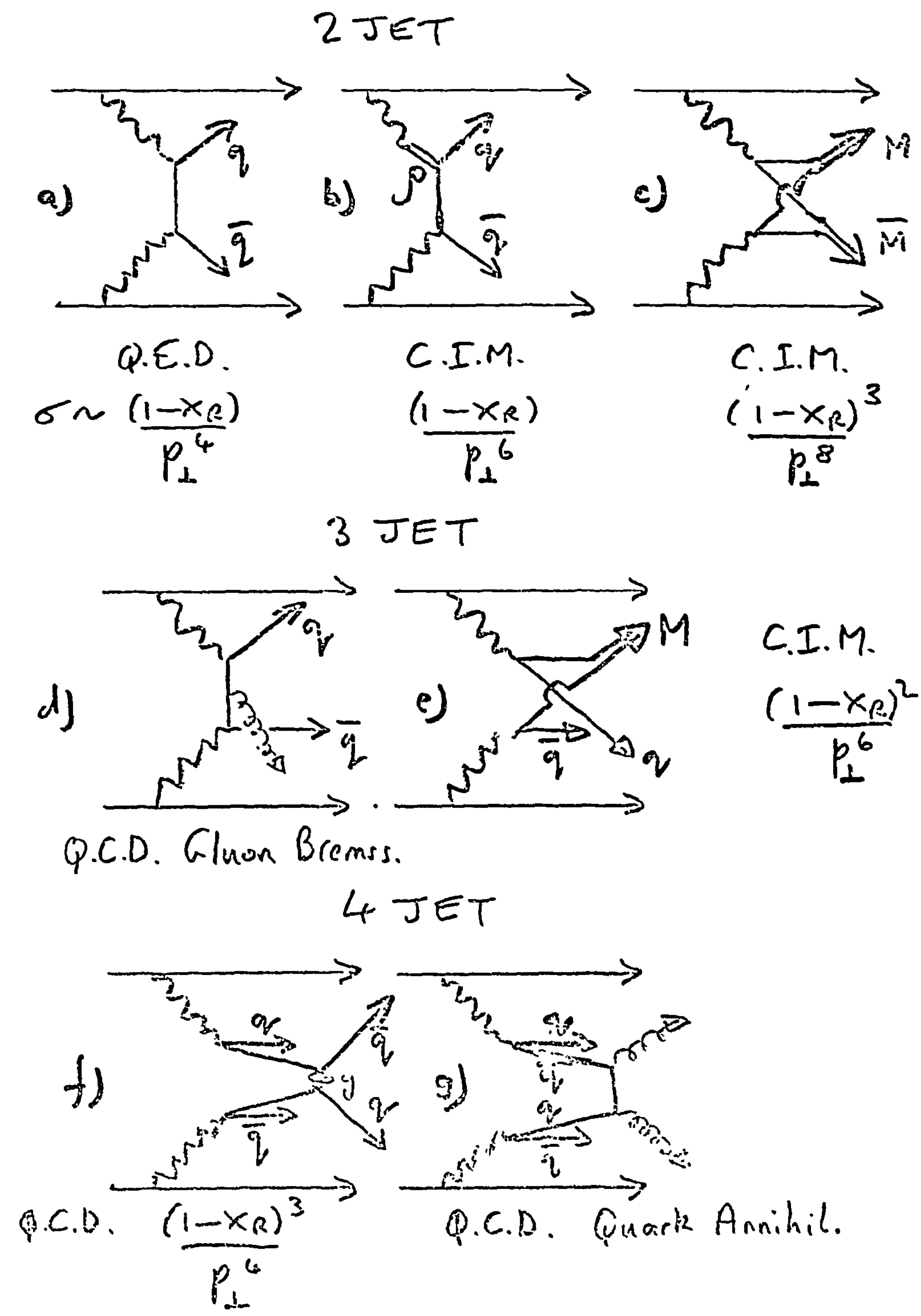

Figure 1 : Jet Physics in γγ Collisions

$$d\sigma(e^+e^- \to e^+e^-q\bar{q}) = R_{\gamma\gamma}\, d\sigma(e^+e^- \to e^+e^-\mu^+\mu^-)$$

where $R_{\gamma\gamma} = 3 \sum_i Q^4_i = 34/27 \qquad i = u,d,s,c$

Q_i = quark charge.

Defining $x_R = E^{quark}/E = E^{JET}/E$ (E = beam energy) and $\theta = \theta^{quark} = \theta^{JET}$ = polar angle to the beams, the differential cross-section for $x_R \sim 1$ is given by[1]:

$$\frac{d^2\sigma}{d\Omega\, dx_R} \simeq \frac{4\, R_{\gamma\gamma}}{s} \left(\frac{\alpha^2}{\pi}\, \ell n\, \frac{E}{m_e}\right)^2 \frac{(1 - x_R)}{x^3_R}\; \frac{(1 + \cos^2\theta)}{\sin^4\theta} \qquad (1)$$

where α = fine structure constant

$s = 4E^2$

Eq. (1) may be compared with the corresponding differential cross-section for the 1γ process:

$$e^+e^- \to q\bar{q} \to 2 \text{ jets}$$

which is:

$$\frac{d\sigma}{d\Omega} = \frac{R_\gamma \alpha^2}{4s}\; (1 + \cos^2\theta) \qquad (2)$$

where $R_\gamma = 3\Sigma Q_i^2 = 10/3 \qquad i = u,d,s,c$

Separation of the 1γ and 2γ processes will be most difficult for large values of x_R. Integrating Eq. (1) over the range $0.8 < x_R < 1.0$ and taking the ratio to Eq. (2) gives:

$$r = \frac{\frac{d\sigma}{d\Omega}^{2\gamma}}{\frac{d\sigma}{d\Omega}^{1\gamma}}\Bigg|_{x_R > 0.8} = 1.89 \times 10^{-2} \left(\alpha\; \ell n\, \frac{E}{m_e}\right)^2 \frac{1}{\sin^4\theta}$$

r is plotted as a function of θ^{JET} in Figure 2.

At beam energies of 15, 70 GeV, r = 1 at angles of 102, 109 mrad so the "cross over" of the 1γ and 2γ processes occurs at $\theta^{JET} \sim 6^o$ almost independantly of the beam energy. For E = 70 GeV this corresponds to a p_t of the jet of ~ 6 GeV. With $\theta^{JET} > 20^o$ the 2γ cross-section is only 1% of the 1γ. It is interesting to note that the curve in Fig. 2 is independent of the number of quarks, provided these always occur in doublets of charge 2/3, -1/3 and both members of each doublet are either excited, or above threshold. In this case the ratio $R_{\gamma\gamma}/R_\gamma$ has the universal value 17/45.

One may conclude from the above analysis that, providing jets can be identified in the final state, the 2γ background will become negligible for $\theta^{JET} > 20^o$ i.e. within the normal acceptance of a central solenoidal detector. Since however the experimental definition of a "jet" is rather more fuzzy than the theoretical one it is of interest to ask what separation of 1γ and 2γ processes

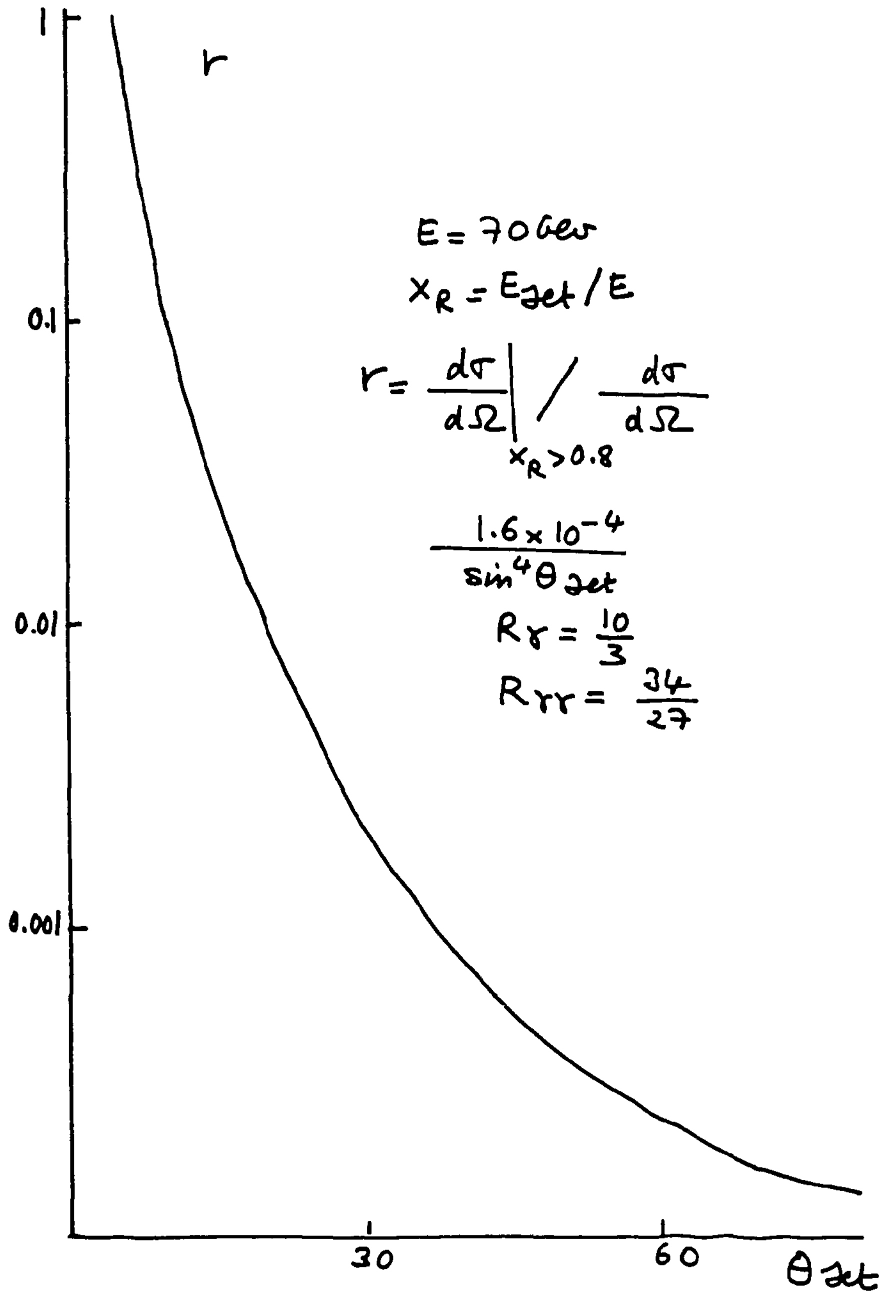
r
1
0.1
0.01
0.001
30
60
θ jet
E = 70 GeV
x_R = E jet / E
r = dσ/dΩ |x_R>0.8 / dσ/dΩ
1.6 x 10^-4 / sin^4 θ jet
Rγ = 10/3
Rγγ = 34/27

Figure 2

can be obtained by use of more straight forward kinematical cuts. Two variables which may be expected to give good discrimination between 1γ and 2γ hadronic events are:

(i) The total observed energy E_{vis}

For 1γ processes this should peak at 2E with a width given by the detector resolution, and a tail extending to lower energies, due to unobserved final state particles. For 2γ processes this variable peaks at low values due to the luminosity function of the γγ collisions which is roughly $\propto \frac{1}{E_{\gamma_1}} \times \frac{1}{E_{\gamma_2}}$ where E_{γ_1}, E_{γ_2} are the lab. energies of the colliding photons.

(ii) The polar angle θ of produced hadrons

For 1γ processes, this is expected to result from the fragmentation of quarks produced with a $1 + \cos^2\theta$ distribution at the quark level, and so to be almost isotropic. In the 2γ process the largest contribution is expected on the basis of VDM to result from quasi-diffractive ρρ scattering, and so to have the most energetic particles at small angles.

In Figures 3 and 4 E_{vis} is plotted for respectively, diffractive and high p_t (two jets as in Fig. 1.a) 2γ processes[9]. In both cases a cut $\theta > 10^o$ is made on the produced hadrons. In Fig. 4 the expected 1γ signal, assuming a resolution of $0.5 \sqrt{E(GeV)}$ for E_{vis} is also shown. It is clear that a cut $E_{vis} > 100$ GeV will reduce the background even from the high p_t 2γ process to negligible levels, while retaining all but a few % at the 1γ signal. More details of the Monte Carlo simulation used for these plots are given in Ref. 9

2.2 Heavy Lepton Production

Here the process of interest is supposed to be 1γ production of a new heavy lepton L of mass greater than the τ. As for the τ, the cleanest experimental signature is expected to be in the purely leptonic decay channels, in particular the eμ channel i.e.

$$e^+e^- \to L^+L^- \to e\mu + 4\nu$$

There are a number of different 2γ processes contributing background:

$$e^+e^- \to e^+e^-\mu^+\mu^-$$
$$e^+e^- \to e^+e^-\tau^+\tau^- \to e^+e^-\ e\mu + 4\nu$$
$$\text{or} \to e^+e^-\ \mu\mu + 4\nu$$
$$e^+e^- \to e^+e^-\ell^+\ell^- \to e^+e^-\ \mu\mu + 4\nu$$

where ℓ is a heavy lepton with $m_\tau < m_\ell < m_L$.

Backgrounds also arise from 1γ production of lighter heavy leptons:

$$e^+e^- \to \tau^+\tau^- \to e\mu + 4\nu$$
$$e^+e^- \to \ell^+\ell^- \to e\mu + 4\nu$$

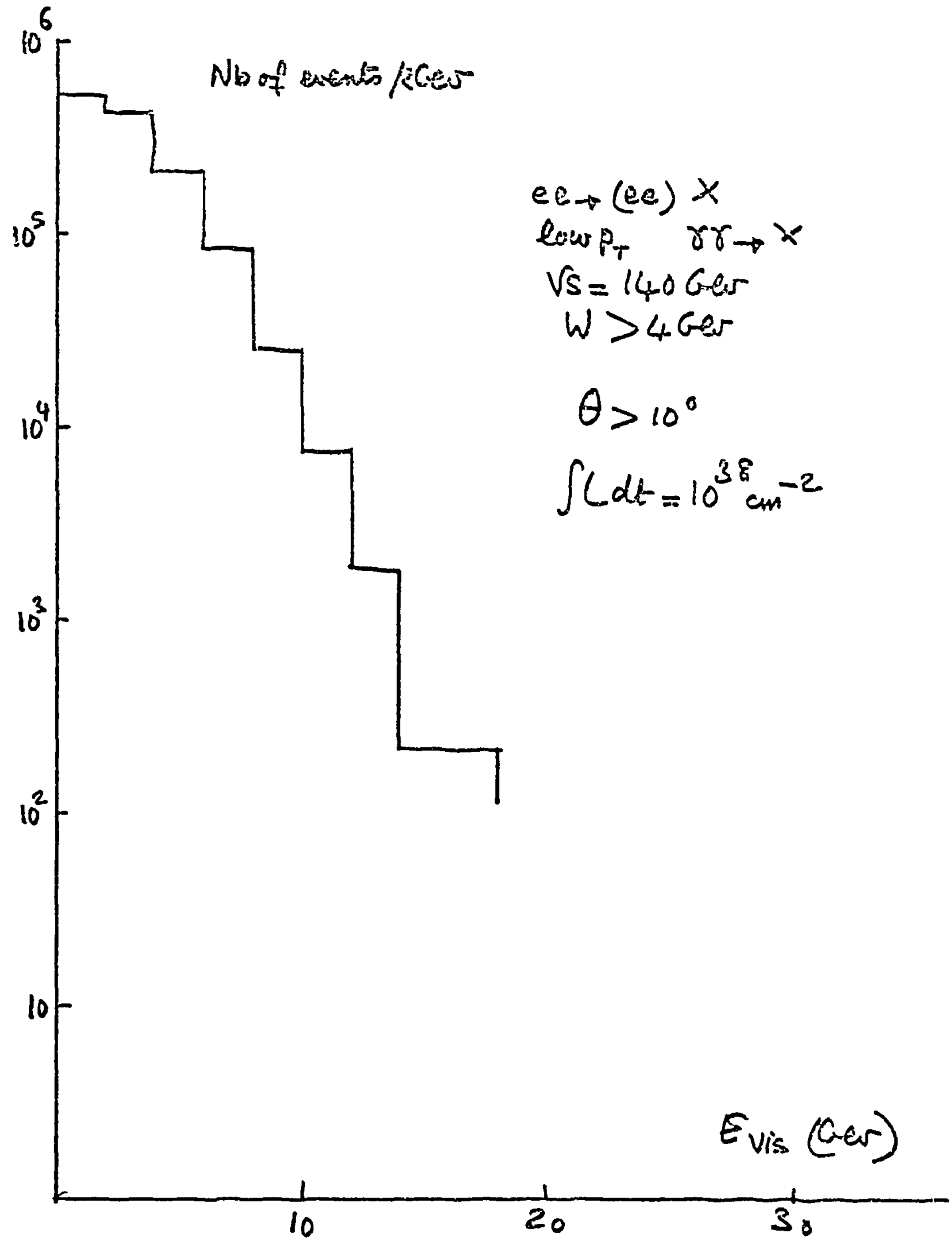
Nb of events/2GeV
ee→(ee) X
low p_T γγ→X
√s = 140 GeV
W > 4 GeV
θ > 10°
∫L dt = 10^38 cm^-2
E vis (GeV)
10^6
10^5
10^4
10^3
10^2
10
10
20
30

Figure 3

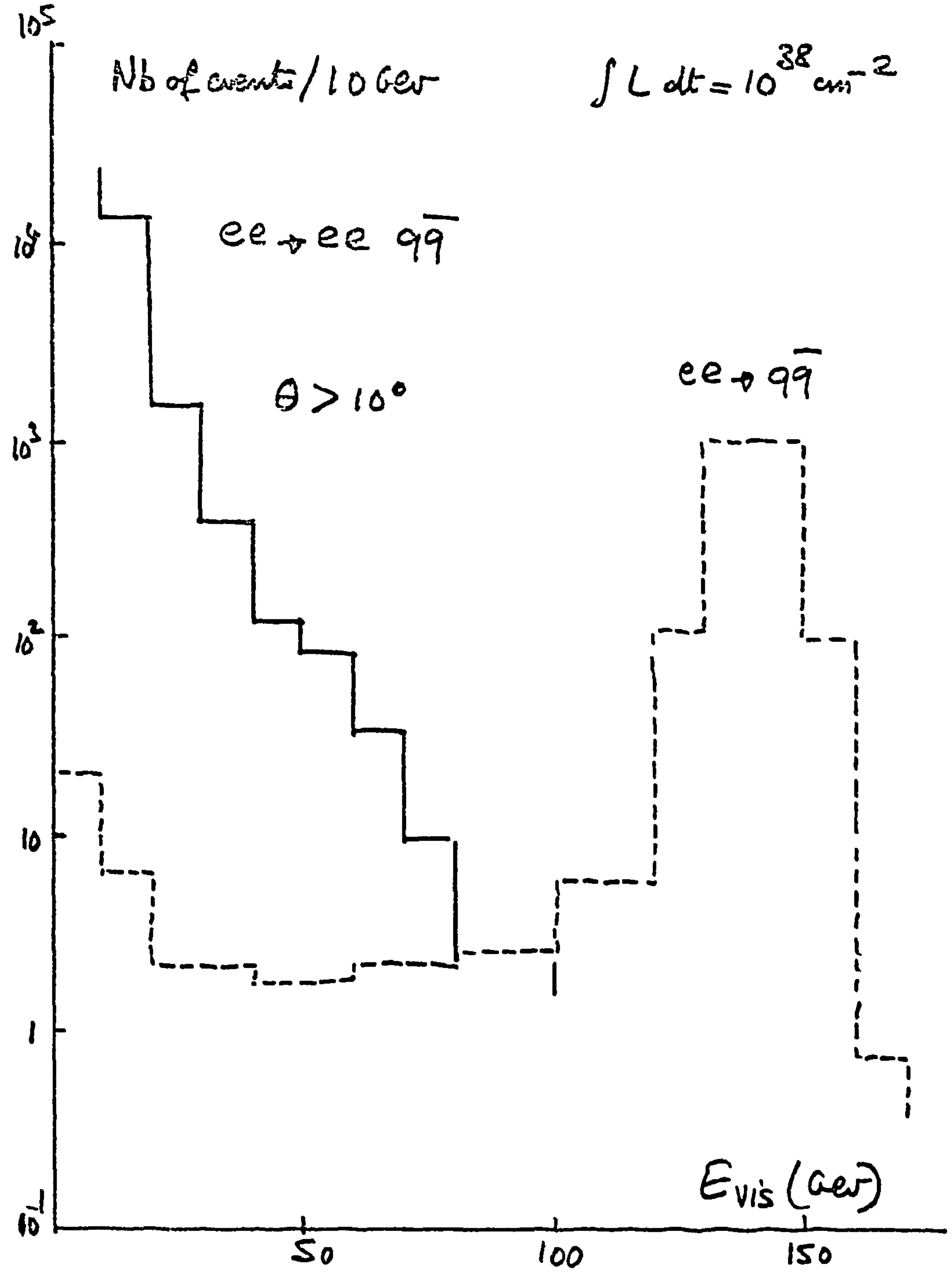
Nb of events/10 GeV
$\int L\,dt = 10^{38}\,cm^{-2}$
ee → ee $q\bar{q}$
θ > 10°
ee → $q\bar{q}$
10^5
10^4
10^3
10^2
10
1
10^{-1}
50
100
150
E_{vis} (GeV)

Figure 4

Because of the large energy carried away by neutrinos, E_{vis} is no longer a useful parameter in separating background. The problem is illustrated in Fig. 5 where the 1γ production of a 40 GeV heavy lepton is compared to the 2γ background from $e^+e^- \to e^+e^-\mu^+\mu^-$[9]. The μμ signature is used and $E_{vis} = E_{\mu^+} + E_{\mu^-}$. Cuts $\theta_\mu, \theta_\mu > 10^o$ are used to suppress the 2γ background, but even so, the heavy lepton signal is buried by some two orders of magnitude under the background.

This problem has been studied in some detail at PEP/PETRA energies by Vermaseren[10]. To separate the $e^+e^- \to e^+e^-\mu^+\mu^-$ background, where an e and a μ are unobserved, use can be made of strong peaking of the unobserved electron in the beam direction. Suppose that the e^+ and μ^- are observed, the e^- and μ^+ being considered "missing" whether or not they are within the acceptance of the apparatus. The polar angle of the missing momentum vector can be calculated from the kinematical variables of the observed particles:

$$\cos\theta^{miss} = \frac{P_L^{miss}}{E^{miss}} = -\frac{(p_{e^+} \cos\theta_{e^+} + p_{\mu^-} \cos\theta_{\mu^-})}{2E - E_{e^+} - E_{\mu^-}}$$

This variable is plotted for E = 15 GeV, M_L = 5 GeV, in Fig. 6[10]. Making a cut $|\cos\theta^{miss}| < 0.3$ retains all the heavy lepton signal. In most cases when $|\cos\theta^{miss}| < 0.3$ either the e^- and/or the μ^+ will also be seen in the detector so the background level will in fact be even lower than shown in Fig. 6. However, scaling to LEP energies, the 2γ signal will be relatively ~20 times higher, corresponding to a signal/background ~1/1 on the peak of the heavy lepton signal. As noted above the background level will certainly be suppressed further by observation of the e^- or μ^+. The background level can also be estimated by taking different charge combinations. With $e^+\mu^+$, $e^-\mu^-$ identical distributions to $e^+\mu^-$ should be obtained for the background contribution.

To separate the channels:

$$\begin{aligned} e^+e^- &\to L^+L^- \to e\mu + 4\nu \\ &\to \tau^+\tau^- \to e\mu + 4\nu \\ &\to e^+e^-\tau^+\tau^- \to e\mu + (e\mu)_{unseen} + 4\nu \end{aligned}$$

Vermaseren[10] suggests use of the variable p_t^r. If p_t^e (p_t^μ) is the transverse momentum of the e(μ), with respect to the μ(e) direction, p_t is the minimum of p_t^e, p_t^μ. This variable measures the transverse momentum in the heavy lepton decay, and has a kinematic limit determined by the heavy lepton mass. In Fig. 7 $\frac{d\sigma}{dp_t^r}$ is shown for E = 15 GeV and heavy lepton masses of 1.8, 5, 10, 14 GeV. Other cuts are detailed in Ref. 10. Also shown is the contribution from the $e^+e^-\tau^+\tau^-$ final state. Remembering that this signal will be some 20 times higher at LEP energies one cannot be too optimistic as to the possibilities of making a clean separation. 2γ production of intermediate mass heavy leptons ℓ will further complicate the situation.

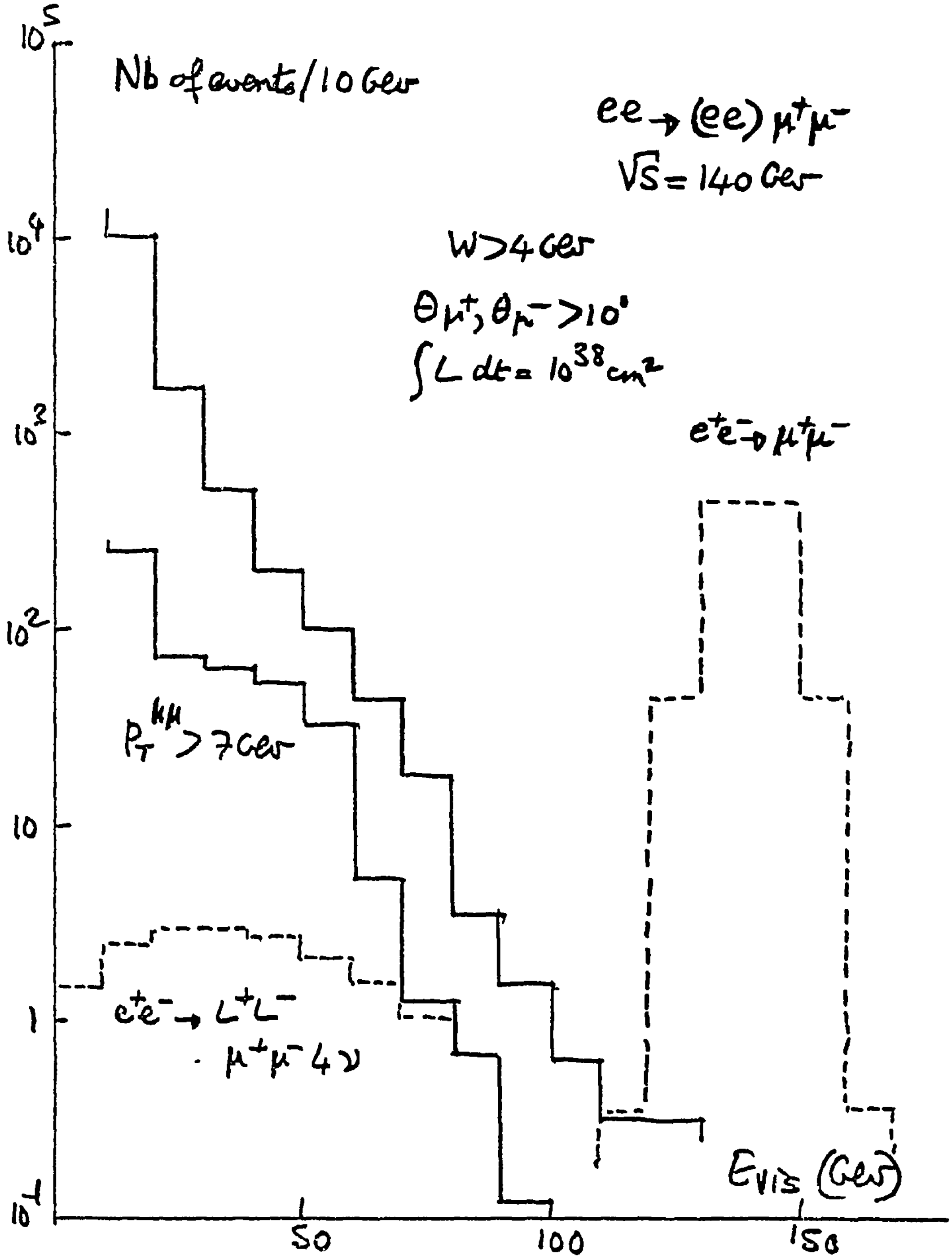
Nb of events/10 Gev
ee → (ee) μ+μ-
√S = 140 Gev
W > 4 Gev
θμ+, θμ- > 10°
∫L dt = 10^38 cm²
e+e- → μ+μ-
P_T^μμ > 7 Gev
e+e- → L+L-
· μ+μ- 4ν
E_VIS (Gev)
50
100
150
10^5
10^4
10^3
10^2
10
1
10^-1

Figure 5

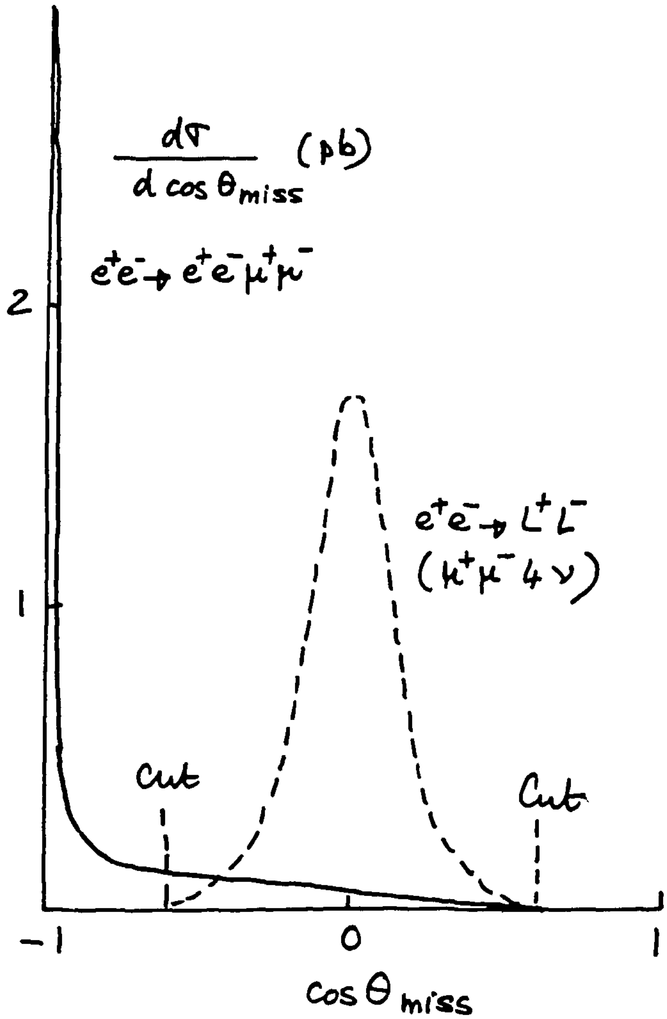

$\frac{d\sigma}{d\cos\theta_{miss}}$ (pb)
$e^+e^- \to e^+e^-\mu^+\mu^-$
2
1
$e^+e^- \to L^+L^-$
$(\mu^+\mu^- 4\nu)$
Cut
Cut
-1
0
1
$\cos\theta_{miss}$

Figure 6

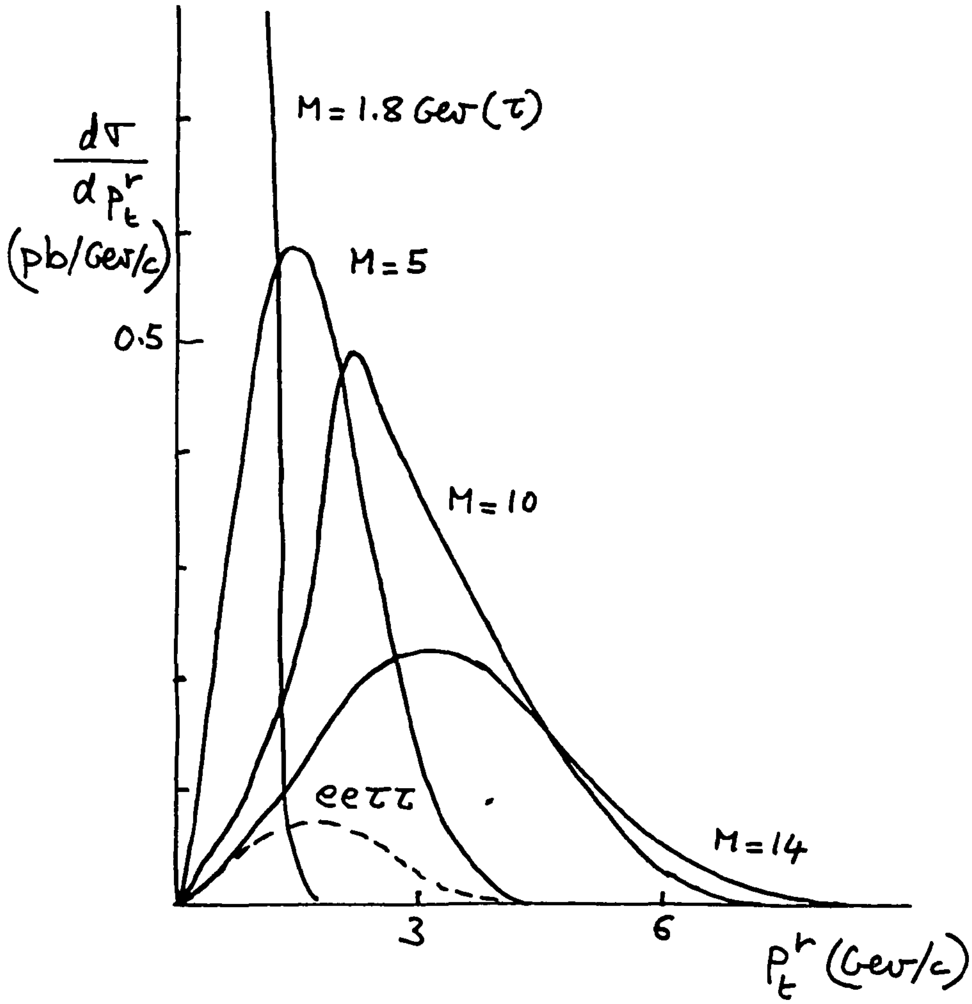

Figure 7

In conclusion more work must be done and more ideas are needed before a clear separation of heavy lepton events from various backgrounds can be expected at LEP energies. The existence of such leptons could no doubt be established by looking for thresholds in the energy dependence of the $e\mu$ signal. To produce clean event samples for more detailed studies seems more difficult.

3. 2γ Physics

3.1 Jet Production

A large number of different processes leading to jets in the final state are expected in 2γ collisions. Some of these processes are shown in Fig. 1[1]. The characteristic x_R and p_t behaviour of the produced jets is indicated. All reactions except that in Fig. 1.c) which corresponds to diffractive $\rho\rho$ scattering in the VDM model, have two jets at high p_t, accompanied by 0, 1 or 2 jets in the beam directions. The p_t behaviour of some of the processes is shown in Figs 8, 9 for E = 15, 70 GeV[1,2]. $E p_t^4 \frac{d\sigma}{d^3p^{jet}}$ is plotted versus p_t for $\theta^{jet} = 90^o$. The already mentioned leading behaviour of the QED graph of Fig. 1.c) is evident. Of particular interest is the 1st order QCD graph of Fig. 1.d) which leads to a 3-jet event. The contribution is comparable to that of the QED graph, and dominates the competing C.I.M. (Constituent Interchange Model) 3-jet process, for $p_t^{jet} > 10$ GeV, E = 70 GeV (Fig. 9). The interest of this process is that a single gluon jet should be produced, clearly separated from the quark jets, so that the properties of the gluon fragmentation function may be directly studied. Another interesting point is the absolute cross-section of the QED graph. As pointed out in P. Landshoff's review, this is 2.5 times larger in the integer charge (Han Nambu) model than in the fractionally charged (Gell-Mann Zweig) model and should allow an easy experimental discrimination between these two models.

All the processes in Fig. 1 have a common experimental signature, two jets should be observed, co-planar with the beams, but in general non-collinear. In addition there may be further jets along the beam pipes. Because of the γγ luminosity function, generally $E_{vis} << 2E$, making the experimental identification of the jets more difficult than in 1γ reactions. To disentangle the different topologies good acceptance near the beam pipes, and double tagging to give kinematically constrained events will be needed. The jets themselves, however, particularly from the leading QED graph, should be evident even without tagging. In fact a clear separation of the 2-jet process, Fig. 1.a), from the diffractive process, Fig. 1.c), can already be seen at the level of the single hadron inclusive distributions, in the Monte Carlo studies of Ref. 5, when suitable cuts are made. This is shown in Fig. 10, where the number of charged tracks is plotted versus their momentum for the QED ($q\bar{q}$) and diffractive ($\rho\rho$) processes.

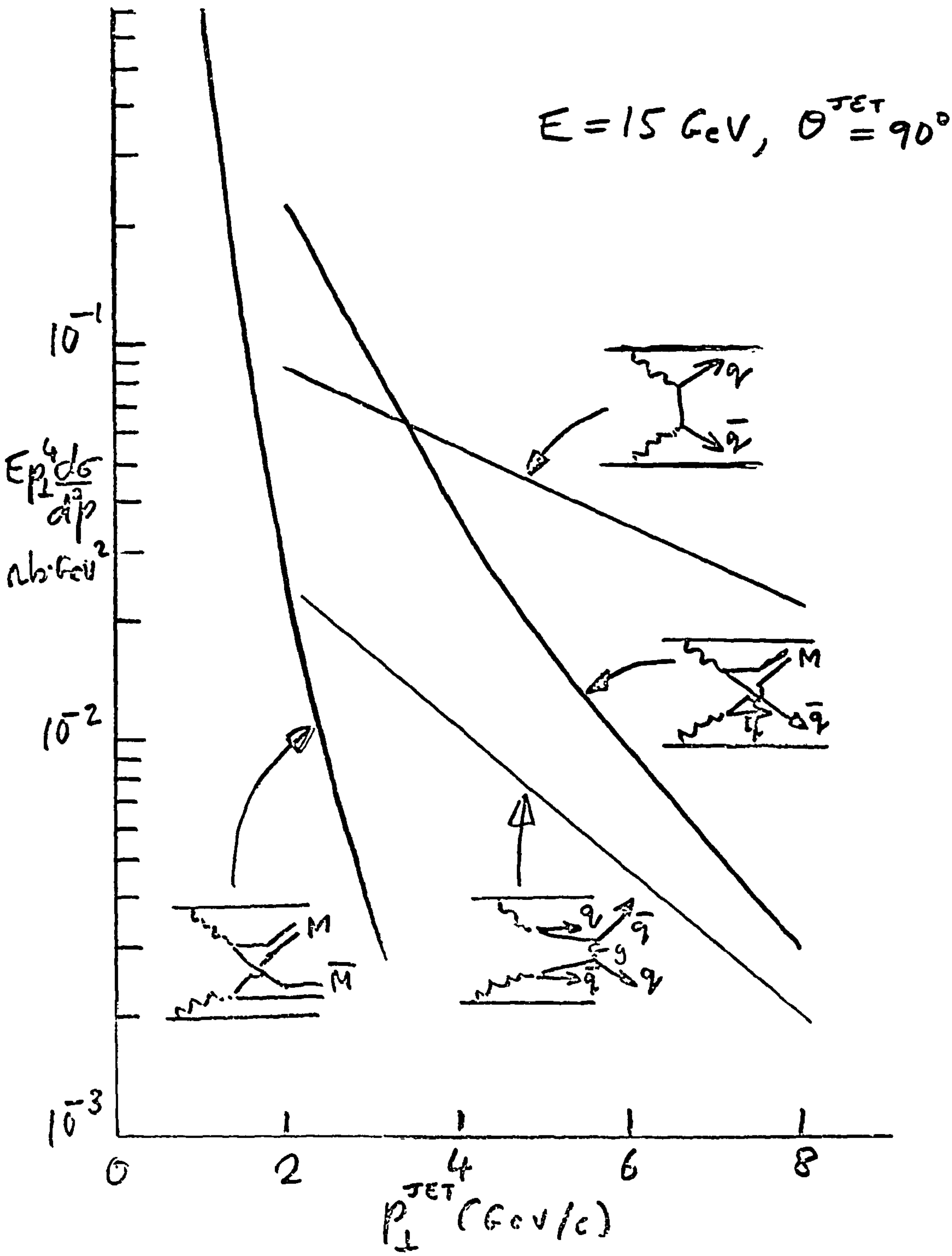

Figure 8 : Jets in γγ collisions. Brodsky, Gunion, DeGrand, Weis P.R.L. 41 (1978) 672

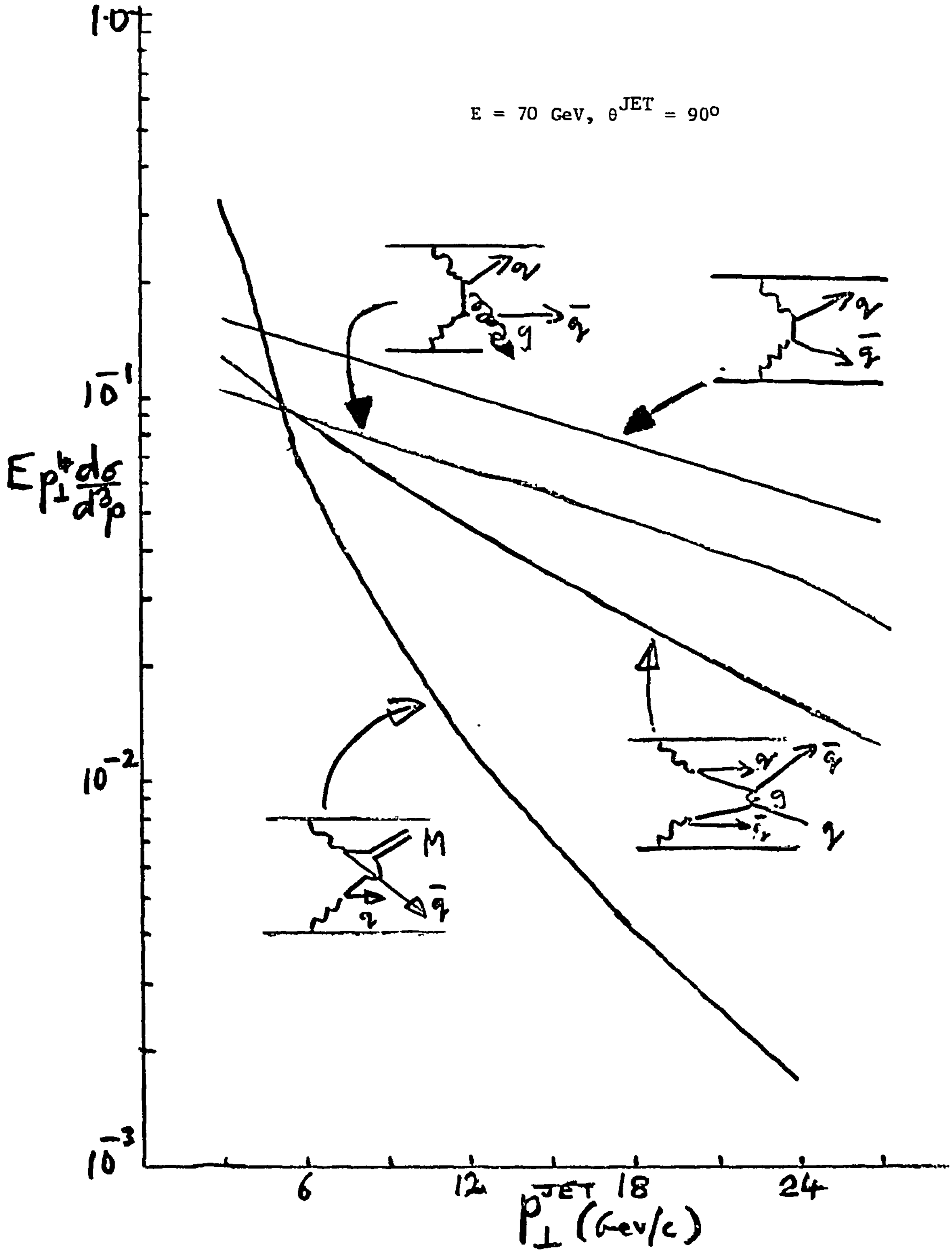

Figure 9 : T. DeGrand. ECFA/LEP 37

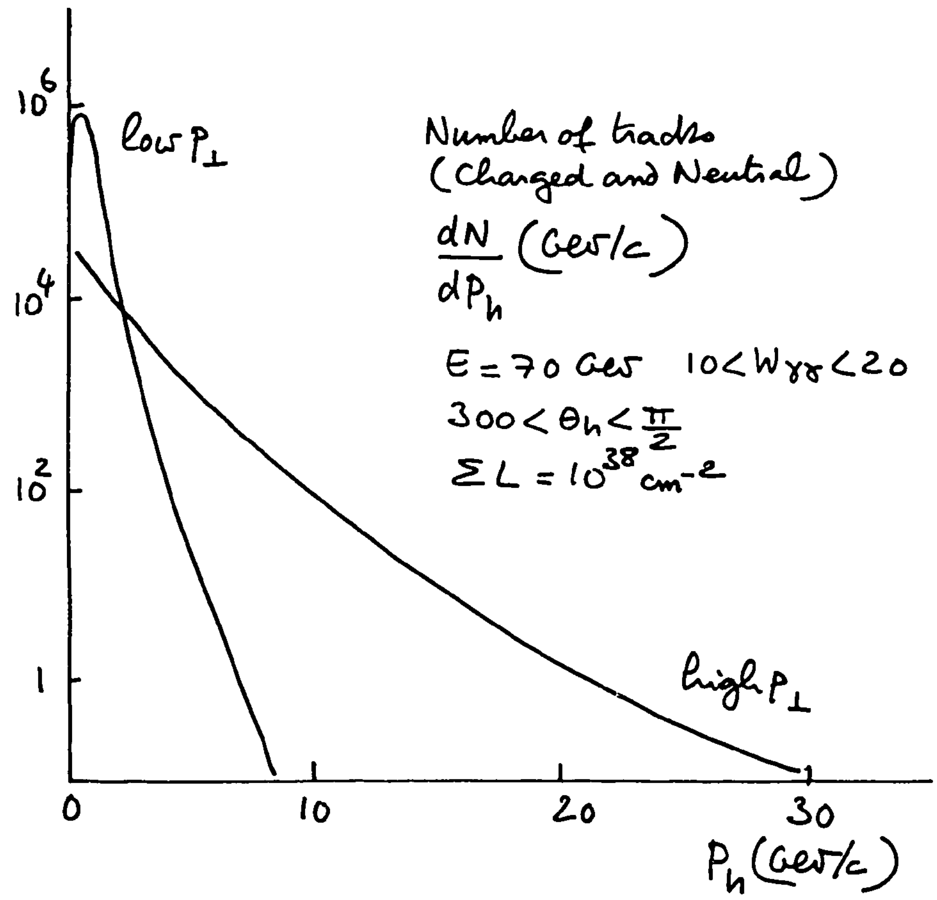

Figure 10 : Separation of high p_t and low p_t 2γ processes from single particle inclusive distributions. M. DAvier, ECFA/LEP 26

3.2 Deep Inelastic γγ Scattering

The physical interest of this process, as a particularly clean test of quark parton and QCD ideas, has been stressed in Landshoff's review. The numbers of events which may be expected above the kinematical region accessible to PEP and PETRA, for an integrated luminosity of $L = 10^{38}\ cm^{-2}$ and $E = 70$ GeV are:

$Q^2 (GeV/c)^2$	$W_{\gamma\gamma}$ = 10 – 20 GeV	20 – 50 GeV
1 – 25	265	850
25 – 100	15	7
> 100	5	10

These figures assume a 5% double tagging efficiency and equal contributions from the box diagram discussed by P. Landshoff, and a VDM contribution which is expected to dominate when $x = \frac{Q^2}{Q^2 + W^2_{\gamma\gamma}} \simeq 0$. Over 10^3 events are expected, which should be sufficient to test the two most interesting theoretical predictions:

- the shape of $F_2(x)$
- the rise $\propto \ln Q^2$ in $F_2(x)$ near $x = 1$.

3.3 Production of C = +1 Mesons

γγ collisions give a unique opportunity to study the direct production of C = +1 states, via the process

$$e^+e^- \to e^+e^-\gamma\gamma \to e^+e^-X$$

where X is a C = +1 meson, e.g. π^o, η^o, η', η_c, χ, η_b, η_t, ... This method has the advantage, over scanning for new states with $J^{PC} = 1^{--}$, in the annihilation channel, that a single run at the maximum beam energy makes available the entire spectrum of C = +1 states to which the machine is sensitive. No time-consuming and rather hazardous (if the states are very narrow) energy scanning is needed. However, if the states are narrow, the available γγ luminosity at any given mass is rather low. Consider for example η_c and η_b states with parameters:

$$\eta_c\ ;\ M = 2.8\ \text{GeV},\ \Gamma_{\gamma\gamma} = 10\ \text{keV}$$
$$\eta_b\ ;\ M = 9.2\ \text{GeV},\ \Gamma_{\gamma\gamma} = 20\ \text{keV}$$

The total cross-sections for production of these states using beam energies of 15, 70 GeV are, in pb:

E(GeV)	η_c	η_b
15	104 (116)	2.0 (2.0)
70	265	9.4

The cross-sections were calculated in the DEPA (Double Equivalent Photon Approximation)[11]. The bracketed numbers are the result of an exact Feynman diagram calculation[12]. On the assumption of an integrated luminosity of $L = 10^{38}\ cm^{-2}$

and 5% double tagging efficiency, the following number of events are obtained:

η_c	η_b
1330	50

Whether these represent observable signals depends on the level of background underneath the resonance peaks. The widths of the latter are determined by the experimental resolution in the $\gamma\gamma$ effective mass, $W_{\gamma\gamma}$. This is given, for production of the resonance at rest in the lab. system, by:

$$\sigma_{W_{\gamma\gamma}} = 2E \sqrt{\frac{1}{2}\left(\frac{\sigma E}{E}\right)^2 + \frac{1}{2}\left(\frac{\sigma E'}{E'}\right)^2} \qquad (3)$$

The dependence of $\sigma_{W_{\gamma\gamma}}$ on the rapidity of the produced state is weak, so only a small error is made by using Eq. (3). $\sigma E/E$ is determined by the beam energy spread in the machine, and is typically ~ 10^{-3} [13]. The best value that can be expected for $\sigma E'/E'$ is that obtained by using NaI detectors for the scattered electrons[14]:

$$\frac{\sigma E'}{E'} = \frac{0.02}{(E')^{1/4}} \simeq 7.0 \times 10^{-3} \qquad (E' \simeq 70 \text{ GeV})$$

so the error on E' is the dominant one and

$$\sigma_{W_{\gamma\gamma}} \simeq \sqrt{2}\, E\, \frac{\sigma E'}{E'} \simeq 900 \text{ MeV } (E = 70 \text{ GeV})$$

Defining the resonance peak by a region $\pm\, 2\sigma_{W_{\gamma\gamma}}$ centered on the maximum, the expected number of background events is[11]:

$$N_b = \varepsilon_{DT}\, L_{ee}\sigma_{\gamma\gamma}^{tot} \left(\frac{2\alpha}{\pi}\right)^2 \left(\ln\,(E/m_e)\right)^2 \frac{1}{z}\left(4\,\ln\frac{1}{z} - 3\right) \frac{2\sigma_{W_{\gamma\gamma}}}{E} \qquad (4)$$

where: $z = \frac{M_X}{2E} \ll 1$, ε_{DT} = double tagging efficiency = 0.05, L_{ee} = luminosity = 10^{38} cm^{-2} s^{-1}

Taking $\sigma_{\gamma\gamma}^{tot}$ = 250 nb leads to the following number of background events, and statistical significance for the signals:

	η_c	η_b
Signal	1330	50
Background	6.9×10^4	7.0×10^3
Statistical Significance	5σ	0.6σ

The situation for the η_b may not be quite so pessimistic as these numbers suggest. As will be discussed in the following section, arguments can be given why the tagging efficiency for background events may be considerably less than the simple expression:

$$\varepsilon_{DT} \simeq \ln^2(\theta\ \max/\theta\ \min)/\left(\ln\,(E/m_e)\right)^2,$$

though the signal should not be so suppressed. The signal/noise ratio can also be improved by making cuts on the p_t of the produced hadrons. Those resulting from the resonance decay, coming, for example, from the fragmentation of two wide angle gluons, should extend to higher p_t values than the background which is expected to be predominantly diffractive.

4. Tagging of Scattered Electrons

4.1 Tagging Efficiency

Except in the region very close to $x_e = E'_e/E = 1$ the single tagging efficiency is almost independent of the scattered electron energy E'_e, and is given approximately (within 10%) by the expression

$$\varepsilon_{ST} = \ln \frac{\theta\ \max}{\theta\ \min} \Big/ \ln (E/m_e) \qquad (5)$$

The tagging efficiency in the region near x = 1, (actually where $\frac{(1 - x_e)^2}{x_e} \leq \theta^2$) is given to within ~ 1% by replacing ln (θ max/θ min) by the expression[11]:

$$\ln \left(\frac{\theta\ \max}{\theta\ \min} \cdot \frac{\left[(1 - x_e)^2 + x_e\ \theta^2_{\min}\right]^{\frac{1}{2}}}{\left[(1 - x_e)^2 + x_e\ \theta^2_{\max}\right]^{\frac{1}{2}}} \right) \qquad (6)$$

The definition of tagging efficiency in Eq. (5) is the ratio of the flux of virtual photons at a given value of x_e in the angular region $\theta_{\min} < \theta < \theta_{\max}$ to the flux in the full angular range $0 < \theta < \pi$. It has been pointed out by M. Davier[6] that in processes where the virtual photon couples to the produced hadronic system via the propagator of a light vector meson (ρ, ω, ϕ) the tagging efficiency will be considerably suppressed compared to the value given by Eqs. (5) and (6). In the case when the vector meson propagator is given by $\frac{1}{(1 - q^2/m_\rho^2)^2}$ and the scattered electron angular distribution in the absence of the propagator is $d\theta^2/\theta^2$, the suppression factor may be calculated analytically with the result:

$$S\ (x_e,\ \theta_{\max},\ \theta_{\min}) = \frac{1}{\ln\left(\frac{\theta^2_{\max}}{\theta^2_{\min}}\right)} \left(\ln\left(\frac{\theta^2_{\max}}{\theta^2_{\min}} \cdot \frac{P(x_e,\ \theta_{\min})}{P(x_e,\ \theta_{\max})} \right) + \frac{1}{P(x_e,\ \theta_{\max})} - \frac{1}{P(x_e,\ \theta_{\min})} \right)$$

where $P(x, \theta) = 1 + \frac{xE^2\theta^2}{m_\rho^2}$.

Figure 11 shows S for E = 70 GeV, $\theta_{\min}$ = 10 mr, $\theta_{\max}$ = 100 mr and m_ρ = 0.773 GeV. In the region near $x_e = 1$, S is ≃0.05.

It should be pointed out however, that by no means all hadronic final states are expected to be produced by VDM like coupling to virtual photons. Some exceptions are:

- production of high p_t jets (point-like coupling of both photons)

- deep inelastic photon coupling (point-like coupling at high Q^2 photon)
- heavy C = +1 resonance production. If η_c, for example, is produced via a VDM-type diagram the propagators might be expected to have a mass $M_{J/\psi}^2$ rather than M_ρ^2 and so have a much flatter Q^2 dependence.

For these processes one might hope that the propagator effects would improve the signal/background ratio by suppressing uninteresting diffractive background. However, it should be stressed that it is quite unknown how much of the total $\gamma\gamma$ cross-section is VDM-like and how much point-like, so the curve of Fig. 11 should be treated as a lower limit. It is also interesting to note that the suppression is least important in the region of small x, corresponding to large effective masses of the produced $\gamma\gamma$ system. This is the kinematic region where it is important to have samples of tagged 2γ events to estimate background levels to 1γ processes. Clearly, one of the most interesting quantities to measure in a 2γ experiment, at a very early stage, will be the Q^2 dependence of the total hadronic cross-section at relatively low values of $Q^2 \leq 1$ GeV/c^2 so as to shed light on the VDM versus point-like nature of the coupling of photons to hadrons in 2γ collisions.

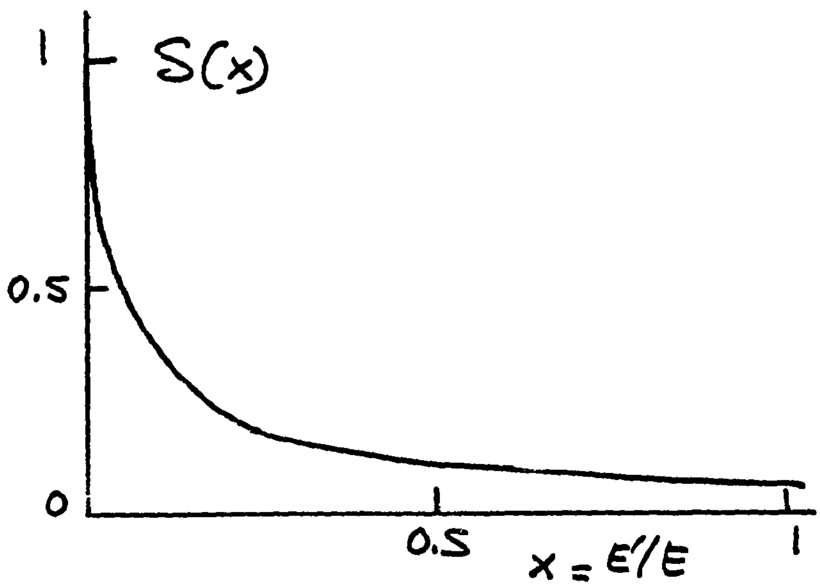

Figure 11 : S(x) = suppression factor of single tagging rate due to ρ propagator $1/(1 - q^2/m_\rho^2)^2$.
E = 70 GeV, 10 ms < θ < 100 ms, m_ρ = 0.773 GeV

4.2 Backgrounds in Tagging

Two different types of background are considered here. The first is an "intrinsic" background resulting from misidentification of forward produced hadrons as electrons. The second results from various external processes that produce electrons at small angles.

In Fig. 12 the x_e distribution of scattered electrons in a typical range of tagging angles 10 mrad < θ < 100 mrad is shown with 3 different assumptions:

Curve B $$\frac{dN}{dX_e} \propto \frac{1 + X_e^2}{1 - X_e} \ln \frac{\theta_{max}}{\theta_{min}}$$

Curve C $\frac{dN}{dX_e}$ given by exact EPA expression[11)]

Curve D $$\frac{dN}{dX_e} \propto \frac{1 + X_e^2}{1 - X_e} \ln \frac{\theta_{max}}{\theta_{min}} S(X_e, \theta_{max}, \theta_{min})$$

i.e. ρ propagator effect from Eq. (7) included.

Also shown in Fig. 12, with the correct relative normalization, is the expected distribution of charged hadrons in the same angular region, from diffractive type 2γ events[5)] where, in almost all cases, the corresponding scattered electrons are in the beam pipe and unobserved (Curve A). It can be seen for small values of X_e, X_h the flux of hadrons is some 2 orders of magnitude higher than the scattered electrons. This can also be seen in Fig. 13 where the ratio of Curve A to Curve D is shown. To reduce the number of false tags to acceptable levels a hadron/electron discrimination factor in the tagging system of the order of 10^3 is needed. If the total energy of the produced hadrons E_{vis} is measured with good efficiency, this background should be largely removed by accepting only events where this directly measured energy agrees with the value $E_{tag} = 2E - E_1' - E_2'$ calculated from the energies E_1', E_2' of the scattered electrons. For the background events, coming predominantly from low energy misidentified hadrons, it is expected that $E_{tag} \gg E_{vis}$.

Some order of magnitude estimates of backgrounds due to various sources of small angle electrons are presented in Table 1. The angular range is 15 mrad < θ < 150 mrad, E = 70 GeV and L = 10^{32} cm^{-2} s^{-1}. The entries are the single tagging rate and the double tagging rate, resulting, in all cases except DBBB, from accidental coincidences. These latter have a rate:

$$f_{DT} = \frac{1}{2} \frac{(f_{ST})^2}{f_B} e^{-f_{ST}/f_B}$$

where f_{ST} is the single tagging frequency and f_B is the bunch crossing frequency = 54 kHz in LEP 70 with 4 bunches in each beam. Also indicated in Table 1 are

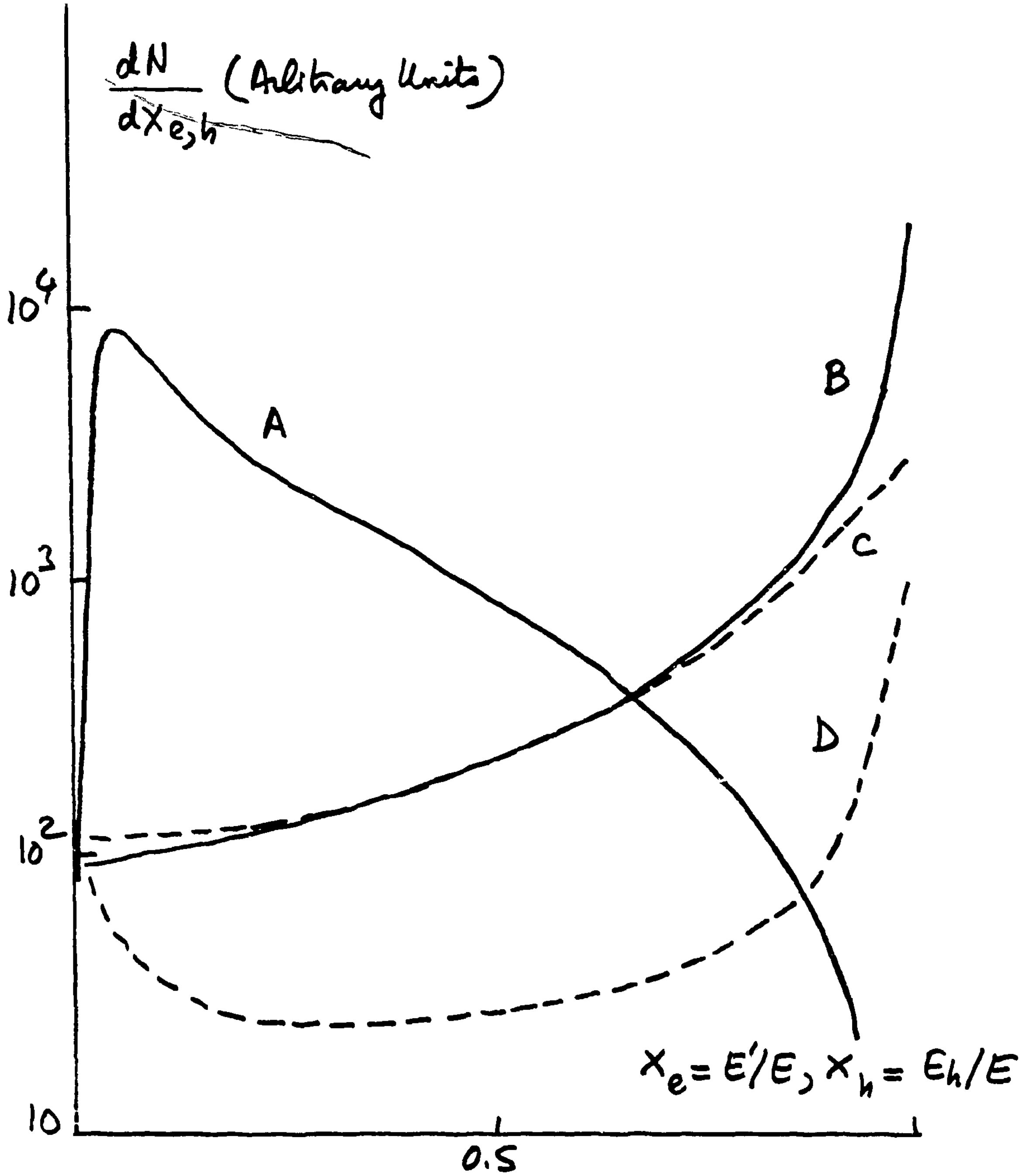

Figure 12 : Comparison of fluxes of charged hadrons and scattered electrons in the tagging region 10 mrad < θ < 100 mrad
$E = 70$ GeV, $W > 4$ GeV

A : hadrons

B : electrons, tagging eff: $\ln \frac{\theta_{max}}{\theta_{min}} / \ln E/m_e$

C : electrons, tagging eff: complete EPA formula[11)]

D : electrons, as B but ρ propagators effect included

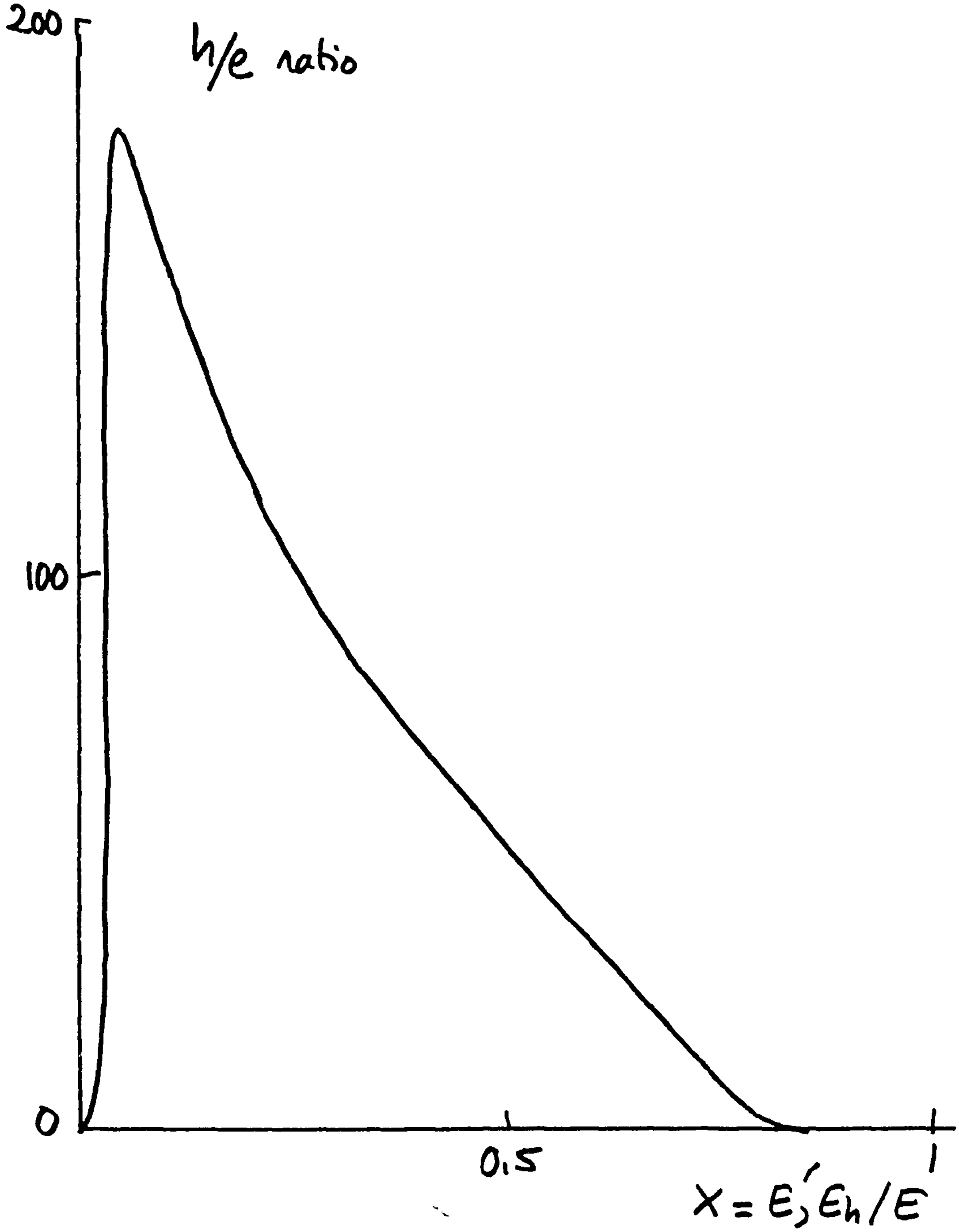

Figure 13 : Ratio of charged hadrons to scattered electrons in the tagging region 10 mrad < θ < 100 mrad.
E = 70 GeV, W > 4 GeV

the main characteristics of the energy spectra of the electrons from the various sources. The bremsstrahlung rates BBB and DBBB, as well as the pair production and Compton rates were taken from formulae and plots given in Ref. 15. The BGB rates were takent from the LEP-70 study[16] and refer to a pressure of 10^{-10} torr.

It can be seen that the most serious background because of its high rate, and because the electrons are quite hard and so cannot be significantly reduced by energy thresholds, is that due to beam-gas bremsstrahlung (BGB). This background consists of electrons, which lose energy in collisions with residual gas in the long straight sections, but remain trapped in the machine until they encounter the strong field gradients of the low-β quadrupoles just before the intersection region, which deflect them into the experimental detectors. The bracketed BGB rates in Table 1 refer to a vacuum of 5×10^{-9} which is typically what is aimed for at PEP and PETRA. Such a vacuum gives a single tag rate of $\sim 1{\cdot}4 \times 10^5$ Hz, 10^6 times larger than the rate from $2\gamma \to$ hadrons, and corresponding to more than two background hits per beam crossing. If 2γ physics is to be possible, or more generally, if any type of tagging is contemplated, the vacuum in the straight sections is of crucial importance. This must be at the 10^{-10} torr level if the BGB rates are to be ~ a few % per beam crossing. Other methods of reducing this background are:

- High Z shielding in the vacuum pipe to absorb electrons not passing close to the interaction point;
- A requirement in the fast trigger, by the use of coincidence matrices, that accepts only electrons pointing from near the interaction point.

5. Detector Design

As discussed in more detail in Refs. 7 and 8, technical limitations impose on the design of 2γ detectors typically four different regions of polar angle θ, relative to the beams, of produced particles. These regions with typical values of θ are:

a)	Beam pipe	$0 < \theta < 10$ mrad
b)	Tagging	$10 < \theta < 100$ mrad
c)	Forward Detector	$100 < \theta < 300$ mrad
d)	Central Detector	$\theta > 300$ mrad

Particles can be detected only in b, c) and d) and there are often dead areas between these regions, due again to various technical constraints.

In Figures 14 - 16 are shown inclusive hadron momentum spectra for the 4 regions a) - d) for the following three processes[5)]

(i) $e^+e^- \to e^+e^-$ + hadrons (low-p_t, $\rho\rho$ scattering)

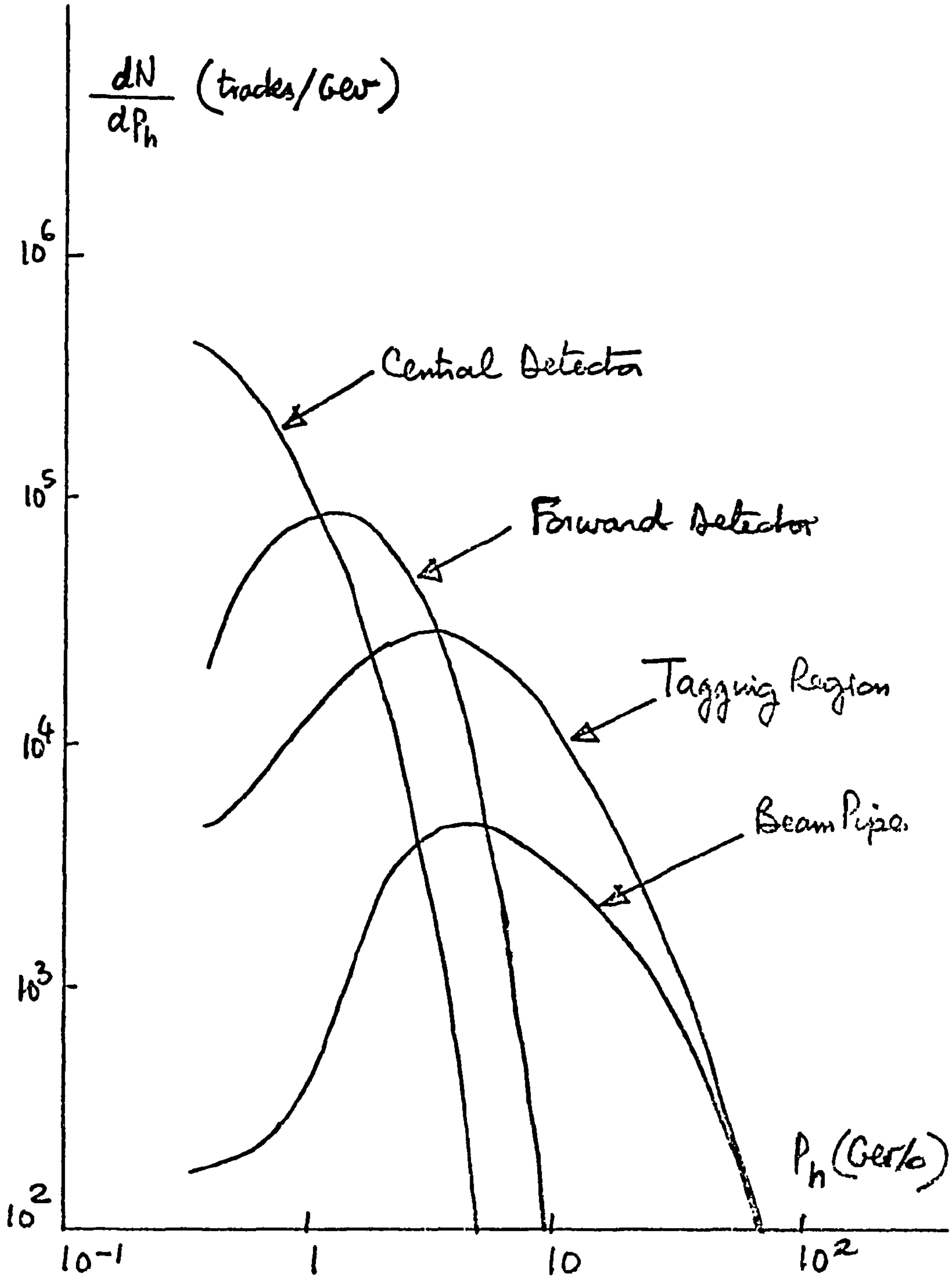

Figure 14 : Inclusive hadron spectra (M. Davier ECFA/LEP 26)
$e^+e^- \rightarrow e^+e^-X$ (low p_t)
charged + neutral, E = 70 GeV, $W_{\gamma\gamma}$ > 4 GeV

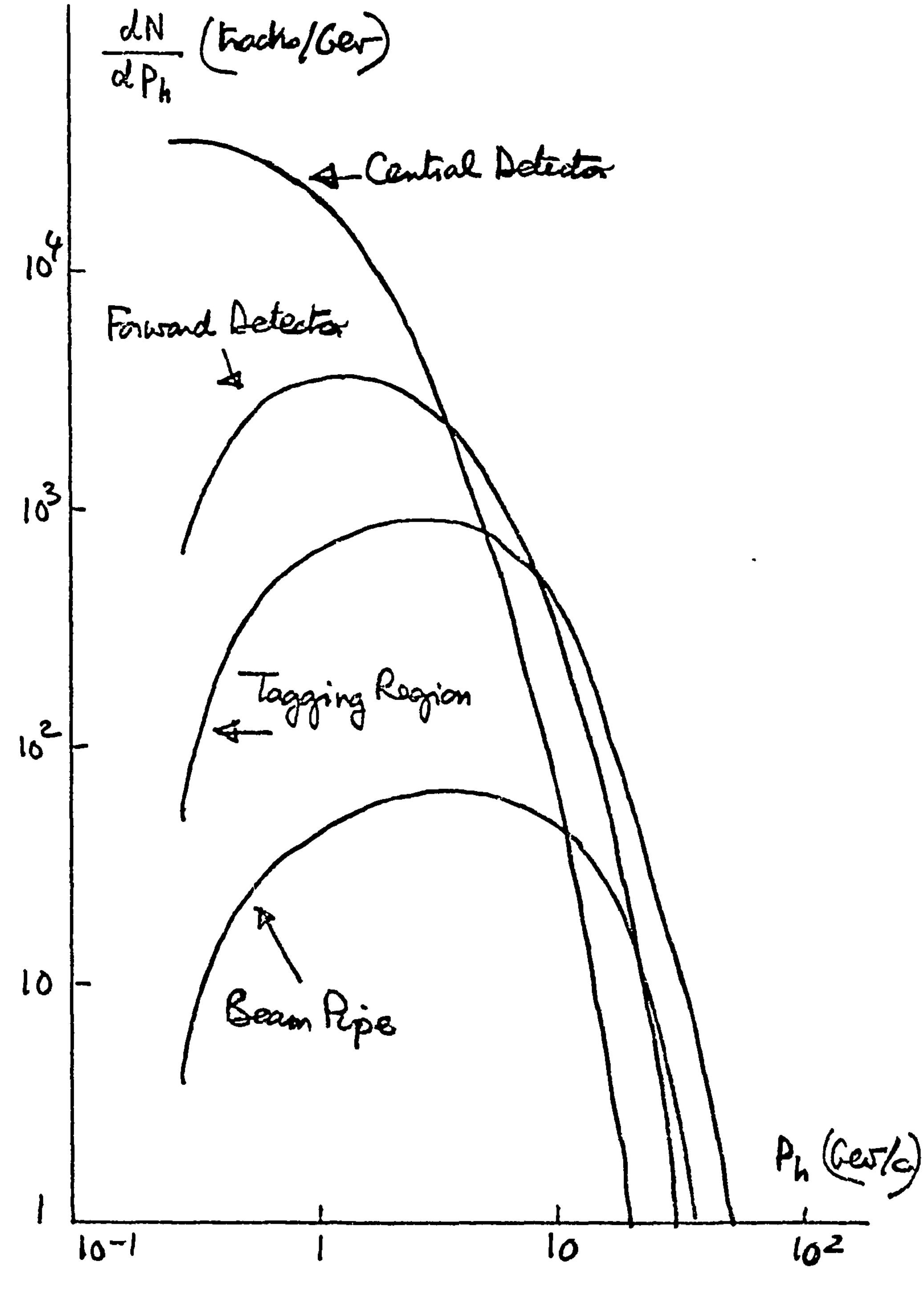

Figure 15 : Inclusive hadron spectra (M. Davier ECFA/LEP 26)
$e^+e^- \rightarrow e^+e^-q\bar{q}$ (high p_t)
charged + neutral, $E \doteq 70$ GeV, $10 < W_{\gamma\gamma} < 20$ GeV

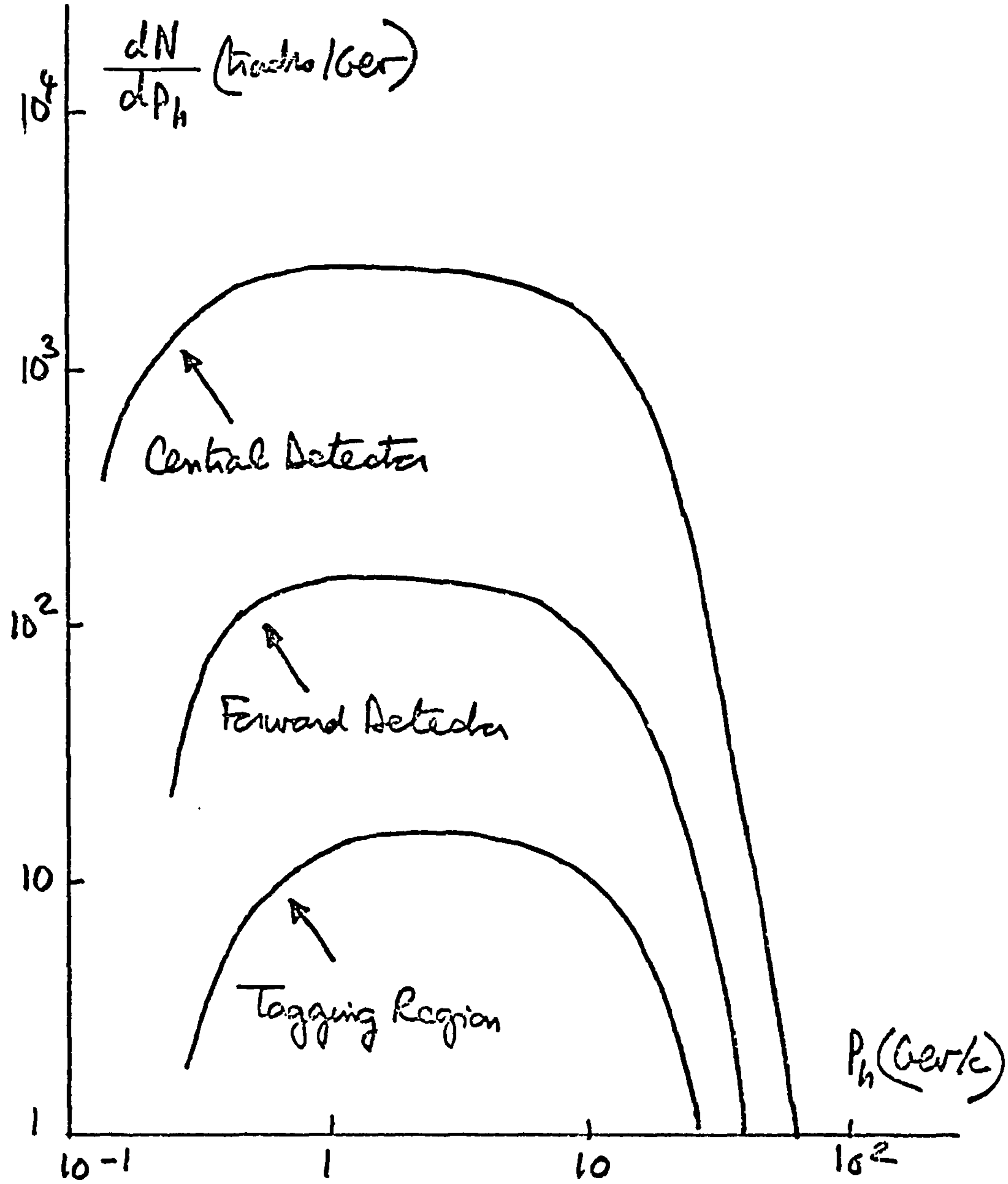

Figure 16 : Inclusive hadron spectra (M. Davier ECFA/LEP 26)
$e^+e^- \rightarrow q\bar{q}$ (annihilation)
Charged + neutral, E = 70 GeV, $\Sigma\mathcal{L} = 10^{38}$ cm^{-2}

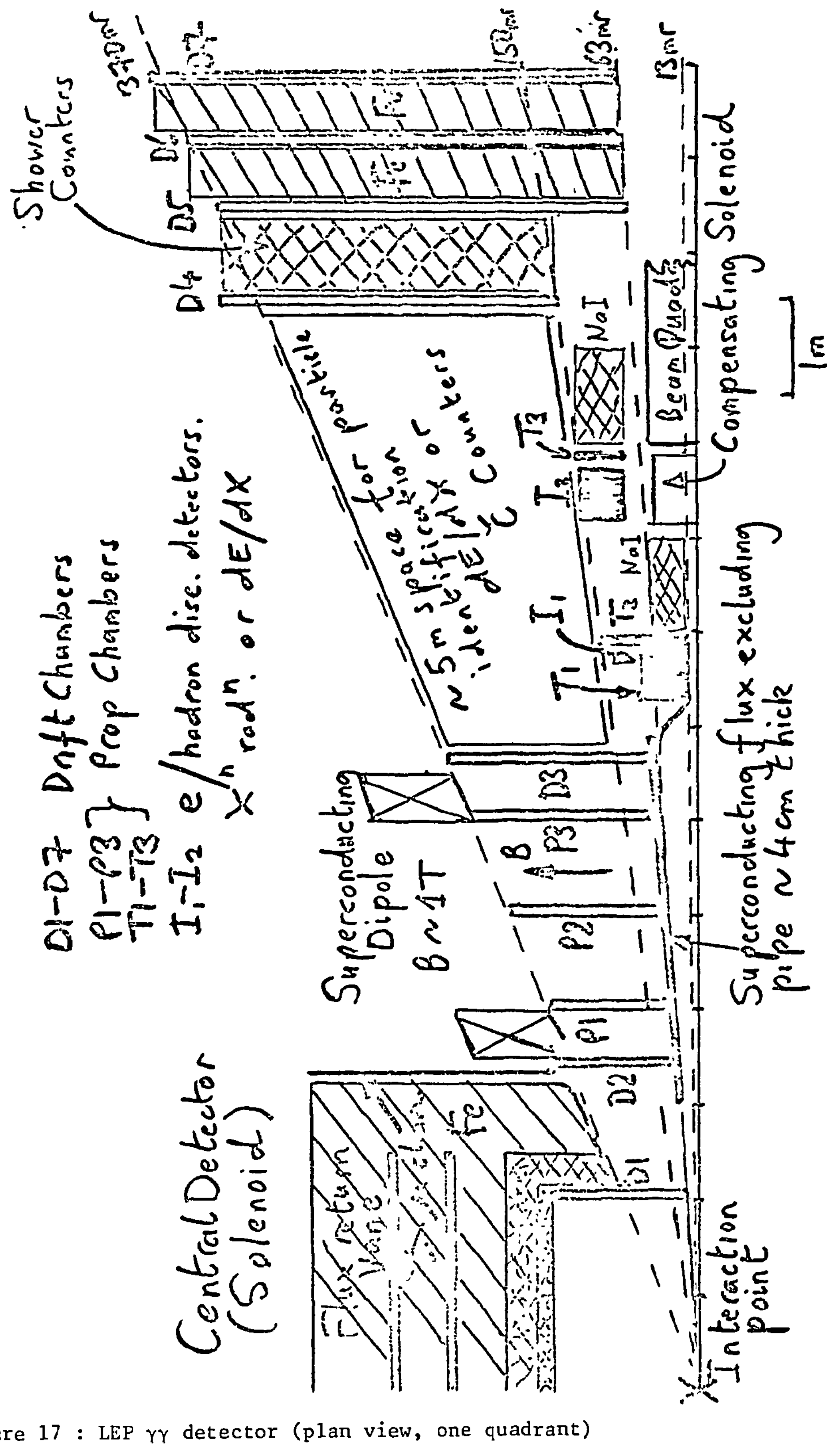

Figure 17 : LEP γγ detector (plan view, one quadrant)

(ii) e^+e^- $e^+e^- + q\bar{q}$ (high p_t, as Fig. 1.a)
$\hookrightarrow$ hadrons

(iii) $e^+e^- \to q\bar{q}$ (annihilation)
$\hookrightarrow$ hadrons

Figures 15 and 16 have the same relative normalization. These plots show two general features of the hadrons from 2γ events:

- the spectra are soft, as compared with those from annihilation events. Even at small angles, in the tagging region, the spectrum peaks around 2 GeV for 70 GeV beam energy;
- large numbers of very soft (< 1 GeV) particles are produced in the central detector region.

These features imply that in the design of 2γ detectors, at least for analyzing the final state hadrons, quite modest magnetic fields are adequate. Another consequence is that particle identification techniques should be aimed at rather low momentum particles. This has not always been the case in previous conceptual designs of 2γ detectors. Thus relativistic ionization rise and time of flight are expected to be important techniques for charged-particle identification.

A possible dedicated detector for 2γ physics, based on the design study in Ref. 17 is snown in Fig. 17. The main features of the detector are summarized in Table 2. Special emphasis is placed on the following points in the design[7]:

- large tagging efficiency
- good e/hadron discrimination in the tagging region (see section 4.2)
- high magnetic field to match electron momentum measurements from bend to NaI energy resolution
- the provision of space for good particle identification (dE/dx, Č, T.o.F.) in the forward direction
- full coverage for neutral detection outside the beam pipe.

Finally, it may be remarked that other design philosophies may have advantages for studying specific physics topics. To improve acceptance, and provide magnetic analysis of momentum down to much lower angles than the detector shown in Fig. 17 one possibility is to use lower magnetic fields, with unshielded beams. These possibilities are discussed at some length in Ref. 8.

Acknowledgements

The work described in this talk owes much to discussions with and contributions from the other members of the 2γ ECFA/LEP subgroup, in particular G. Barbiellini, M. Davier and F. Erne. I am also indebted to K. Kajantie, P. Landshoff and C.H. Llewellyn-Smith for their enlightening remarks on theoretical questions.

Table 1 : Tagging Backgrounds

Process	Single Tag Rate Hz	Double Tag Rate Hz	Electron Energy Range
Signal: $e^+e^- \to e^+e^-$ + hadrons (no propagator suppression, see section 4.1)	0.11	0.015	$4 < E'_e < 67$ GeV (bremss. spectrum)
BBB: $e^+e^- \to e^+e^- \gamma$	11.6	1.2×10^{-3}	" " " " " "
DBBB: $e^+e^- \to e^+e^-\gamma\gamma$	0.01	< 0.002	" " " " " "
BGB: e.g. eco → ecoγ	2.7×10^3 (1.4×10^5)	64 (1.4×10^4)	Flat 0 - 50 GeV
Pair production on synchrotron radiation: $e\gamma \to ee^+e^-\gamma$	~ $10^3 - 10^4$	~ $10 - 10^3$	$1 < E'_e < 100$ MeV (peaked low)
Compton scattering on synchrotron radiation $e\gamma \to e\gamma$	~ 200	~ 0.4	$1 < E'_e < 1000$ MeV (peaked low)

For BGB: $p = 10^{-10}$ torr, in ( ) $p = 5 \times 10^{-9}$ torr   N.B. bunch crossing frequency = 54 kHz

$15 \text{ mrad} < \theta < 150 \text{ mrad}$, $E = 70$ GeV, $L = 10^{32}$ cm^{-2} sec^{-1}

Table 2 : Summary of $\gamma\gamma$ Detector

I	II	III	IV	V	VI
0 ~ 12.5 mr	12.5 - 62. 5 mr	62.5 - 75.8 mr	75.8 - 150 mr	150 ~ 367 mr	> 367 mr
Beam-pipe Dead	Tagging, B = 0 NaI $\sigma_E/E = 0.02/E^{\frac{1}{4}}$ Prop^n chambers π/e disc: 3 layers of X^n rad^n detectors† Length 60 cm π/e rej: 10^3 (2 GeV) e detection eff: $(.97)^3 = 0.91$ (2 GeV) No μ/π disc	Super- conducting pipe Dead	Tagging, horiz. dipole field B ~ 1T $\int$ Bdl = 3 Tm $\sigma p/p = 2 \times 10^{-4}$ p Drift chambers: σ ~ 200 μ NaI, Prop^n ch. as II π/e disc. as II π/K T.o.F. p < 1.5 GeV K/p T.o.F. p < 2.5 GeV (σ_t = 0.2 ns, 30 sep) μ/π disc ~ 1 m Fe few % rej.	B) as Drift Chambers) IV E.M. Shower Detectors Pb-scintillator or liquid A $\sigma_E/E \sim 0.1/\sqrt{E}$ π/K T.o.F. p < 1.6 GeV K/p T.o.F. p < 2.7 GeV π/K/p separation at higher energies dE/dX or C counters in tandem μ/π disc as IV	Solenoid Modest Resolution $\sigma p/p$ ~ 0.01 - 0.03 x p sin θ e.g. CELLO JADE TASSO

† See ref. 18.

References

1) S.J. Brodsky, T.A. DeGrand, J.F. Gunion and J.H. Weis, Phys. Rev. Letters 41 (1978) 672

2) T.A. DeGrand ECFA/LEP 37

3) K. Kajantie, Univ. of Helsinki preprint HU-TFT-78-30

4) C.H. Llewellyn-Smith, Univ. of Oxford preprint 56/78 (1978)

5) M. Davier ECFA/LEP 26

6) M. Davier ECFA/LEP 25

7) J.H. Field ECFA/LEP 28

8) I. Duerdoth, J.H. Field and M. Steuer ECFA/LEP report in preparation

9) M. Davier ECFA/LEP 27

10) J.A.M. Vermaseren 'Signals for Very Heavy Leptons in e^+e^- Annihilation' Purdue Univ. preprint 1978

11) H. Terezawa Rev. Mod. Phys. 45 (1973) 615

12) J.A.M. Vermaseren, J. Smith and G. Grammer Stony Brook preprint ITP-SB-78-3-9 (1978)

13) CERN/ISR-LEP/78-17 p. 175

14) E.B. Hughes XVI Int. Conf. on High Energy Physics Batavia Ill. p 405 (1972)

15) 'Physics with Very High Energy e^+e^- Colliding Beams' L. Camilleri et al. CERN 76-18 1976

16) Ref. 13 above p. 136

17) Proceedings of the 1975 PEP Summer Study LBL-4800, SLAC-190 p. 168

18) J. Cobb et al. Nuc. Insts. Methods 140 (1977) 413